# Compressed Sensing-Based Ultrasound Imaging for Faster Acquisition and High-Quality Images

A

Term Paper on Image Processing

Submitted in partial fulfilment of the

Requirements for the award of the Degree of

**BACHELOR OF ENGINEERING**

IN

**COMPUTER SCIENCE &**

**ENGINEERING**

By

**SVN Ramakanth**
**1602-19-733-118**

**Under the guidance of**

**Dr.D. BASWARAJ**

**Department of Computer Science & Engineering**

**Vasavi College of Engineering (Autonomous)**

**(Affiliated to Osmania University)**

**Ibrahim Bagh, Hyderabad-31**

**2021-22**

# Abstract

Typical SRUS(Super Resolution Ultra Sound) images are reconstructed by localizing ultrasound microbubbles (MBs) injected into a vessel using normalized 2-dimensional cross-correlation (2DCC) between MBs signals and the point spread function of the system. However, current techniques require isolated MBs in a confined area due to inaccurate localization of densely populated MBs. To overcome this limitation, we developed the L1-homotopy based compressed sensing (L1H-CS) based SRUS imaging technique which localizes densely populated MBs to visualize microvasculature in vivo. Methods: To evaluate the performance of L1H-CS, we compared the performance of 2DCC, interior-point method-based compressed sensing (CVX-CS), and L1H-CS algorithms. Localization efficiency was compared using axially and laterally aligned point targets (PTs) with known distances and randomly distributed PTs generated by simulation. We developed post-processing techniques including clutter reduction, noise equalization, motion compensation, and spatiotemporal noise filtering for in vivo imaging. We then validated the capabilities of the L1H-CS-based SRUS imaging technique with high-density MBs in a mouse tumor model, kidney, and zebrafish dorsal trunk, and brain. Compared to 2DCC and CVX-CS algorithms, L1H-CS achieved faster data acquisition time and considerable improvement in SRUS image quality.

# Table of contents

# Introduction

CONTRAST enhanced ultrasound imaging has been developed using microbubbles (MBs) to provide improved therapeutic outcomes and anatomical and functional information for the diagnosis of disease and preclinical investigations. MBs have been utilized for blood-brain barrier opening and drug/gene delivery by stable and inertial oscillations to increase the permeability of connective tissues in brain vasculature. Targeting specific biomarkers using MBs with functional moieties detects tumor angiogenesis with high specificity using ultrasound imaging. Super-resolution ultrasound (SRUS) imaging technique utilizes the blinking of MBs by compounding thousands of frames to construct micro-vessel images to examine the structural abnormalities and dysfunction of the vessel in various types of organs and leaky vasculature in tumor mass.

Before constructing the SRUS image, the clutter signals of each frame are removed by applying to transmit or post-processing techniques such as pulse inversion, differential imaging, and singular value decomposition (SVD) filtering. Among them, SVD filtering was demonstrated as a suitable processing step to precisely localize MBs in the range of a few micrometers. The normalized 2-dimensional cross-correlation (2DCC) technique is then utilized to localize MBs by comparing detected MBs signals and the point-spread function (PSF) of the ultrasound imaging system.

However, the 2DCC algorithm does not accurately detect densely populated MBs. Recently, compressed sensing (CS) has been introduced as a promising technique to reconstruct original signals from sparsely sampled signals that do not satisfy the Nyquist-Shanon sampling theorem.

In this paper, we present an L1H-CS-based SRUS imaging technique that could reduce both the computational time and the acquisition time of ultrasound image frames for the reconstruction of the SRUS image. Furthermore, clutter reduction, noise equalization, motion correction, and spatiotemporal noise filtering algorithms were developed to perform in vivo imaging.

# Existing Methodologies

## A. 1-homotopy Based Compressed Sensing

Mathematically, detected MBs signals, y, using the ultrasound imaging system have a linear relationship with location,

$$x\ y = \Phi x + e$$

where y and x consist of the one-column vectors reshaped from the 2D matrix by row-wise concatenating the matrix of the original image or the localized results in the unsampled space or pixels respectively. The matrix Φ represents the point spread function (PSF) derived by an imaging system by simulation or actual measurements. e denotes a noise vector. To achieve up-sampled localized results, x, at a measured frame, y, the interior point method utilizes to resolve the L1-norm minimization problem for CS as follows:

$$\text{minimize} : \|x\|_1$$

$$\text{subject to} : x_i \geq 0 \text{ and } \|\Phi x - y\|_2 \leq \varepsilon,$$

To solve the minimization problem efficiently, an alternative method was proposed as follows:

$$minmize : \ \lambda\|x\|_1 + \frac{1}{2}\|\Phi x - y\|_2^2,$$

where λ is a positive weight. Eq. (3) was expanded to build the L1H-CS formulation using the homotopy parameter, ε , as follows :

$$minmize : \ \lambda\|x\|_1 + \frac{1}{2}\|\Phi x - y\|_2^2 + (1-\epsilon)\, u^T x,$$

$$u \ = \ -\lambda sign\,(x) - \Phi^T\,(\Phi x - y)$$

The homotopy method offers a typical framework that can solve an optimization problem by continuously transforming it into a related problem with less computing cost.

## B. Ultrasound Imaging Configuration

For the acquisition of the in-phase and quadrature (IQ) data, we utilized an ultrasound imaging research platform (Vantage 256, Verasonics Inc., Kirkland, WA, USA) with a high-frequency linear array transducer (L35-16vX, Vera sonics Inc., Kirkland, WA, USA). For in vivo imaging, the PSF of MBs was generated as follows:

$$PSF = exp\left(-\left(\frac{(z-c_z)^2}{2\cdot {\sigma_a}^2}+\frac{(x-c_x)^2}{2\cdot {\sigma_l}^2}\right)\right)$$

### C. Post-Processing for in Vivo Super-Resolution Ultrasound Imaging

First, the stacked spatial IQ data are converted into a 2D space-time matrix called Casorati matrix S. The SVD of S was described as follows:

$$S = U\Lambda V^*$$

Then, the filtered signal was reconstructed by:

$$\mathrm{Signal(x,z,t)}_{filtered} = \sum_{i=T_l}^{last} U_i(x,z)\,\Lambda_i V_i(t)$$

To evaluate denoising techniques including SVD, SVD + noise equalization, SVD + noise equalization + NLM filtering, we measured CTR and SNR of denoised images as follows:

$$CTR\ (dB) = 20log_{10}\left(\frac{V_{MBs}}{V_{Tissue}}\right),$$

$$SNR\ (dB) = 20log_{10}\left(\frac{V_{MBs}}{std\,(noise)}\right),$$

## D. Point Target Preparation Using Simulation

To evaluate the performance of localization using 2DCC, CVX-CS, and L1H-CS algorithms, two points aligned along with axial and lateral directions and randomly distributed PTs were generated in simulation. First, two-PTs were constructed at each inter-point distance from 13.75 to 110 μm with a step size of 13.75 μm in axial and lateral directions, respectively. The wavelength in this study was 61.6 μm. We localized these two points using 2DCC, CVX-CS, and L1H-CS algorithms to examine the minimum distance that can be localized in axial and lateral directions

# Results and Discussions

## A. Evaluation of the Localization Techniques Using Two-Point Targets in Simulation

The performance of the localization capability was analyzed by comparing 2DCC, CVX-CS, and L1H-CS based localization techniques. Two-PTs separated by a known distance in axial and lateral directions were used. Figs. 2(a-f) show the minimum distance between two-PTs that can be localized by 2DCC, CVX-CS, and L1H-CS algorithms, respectively. These were overlaid with B-mode images. Blue, green, and red asterisks indicate the locations of localized points by 2DCC, CVX-CS, and L1H-CS, respectively. Black circles indicate the location of simulated points

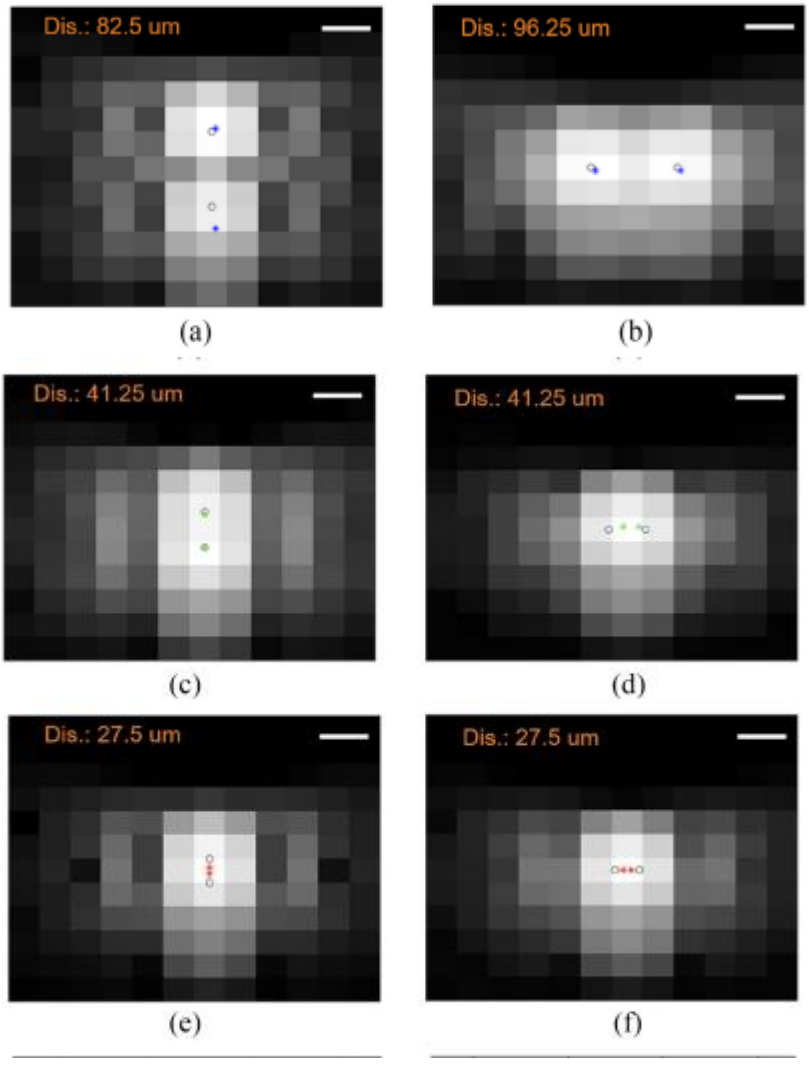

## B. Evaluation of the Localization Techniques Using Randomly Distributed Point Targets in Simulation

We compared the performance of the localization techniques using randomly distributed PTs depending on point density. Figs. 3(a-c) show the representative localization results by 2DCC, CVX-CS, and L1H-CS overlaid with B-mode images of randomly distributed PTs at a density of 55.62 PTs/mm2. Blue, green, and red asterisks indicate localized points by 2DCC, CVX-CS, and L1H-CS, respectively. Black circles indicate the location of simulated points. For randomly distributed PTs at a density of 55.62 PTs/mm2, the average densities with the standard deviation of localized points using 2DCC, CVX-CS, and L1H-CS algorithms were measured as 21.93 ± 1.97, 46.4 ± 2.85, and 50.74 ± 0.62 PTs/mm2, respectively. As shown in the insets of Figs. 3(a-c), overlapped points were localized using CS algorithm, but 2DCC could not localize them. Figs. 3(d-e) show localized PTs density and localization error by 2DCC, CVX-CS, and L1H-CS. The black dashed line in Fig. 3(d) indicates the ideal localization of Pts.' 2DCC algorithm departs from the black dashed line significantly when the density of simulated points reaches 15.89 PTs/mm2 [blue line in Fig. 3(d)]. CS-based algorithms followed the black dashed line closely until the target density increased to 55.62 PTs/mm2 as indicated by the black arrow in Fig. 3(d)

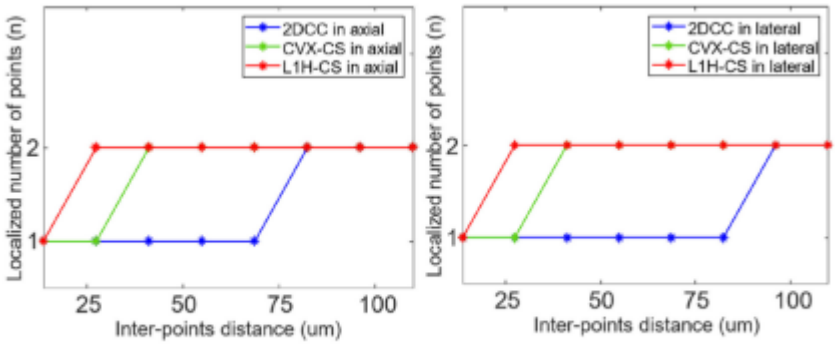


(g) (h)

## C. Evaluation of Post-Processing Techniques Using Images of in Vivo Mouse Tumor Model

After evaluating the localization technique using simulated PTs, we first examined the effects of combinations of post processing techniques including SVD, noise equalization, and NLM filtering to improve CTR and SNR of MBs signals. Figs. 4(a-d) show images before and after applying SVD, noise equalization, and NLM filtering to the data set acquired by ultrasound imaging of in vivo mouse tumor model. To calculate CTR, MBs and tissue signals were collected from the B-mode, SVD, SVD + noise

equalization, and SVD + noise equalization + NLM filtered images. ROIs were selected at the same depth indicated as the orange boxes shown in Fig. 4(b) for all images.

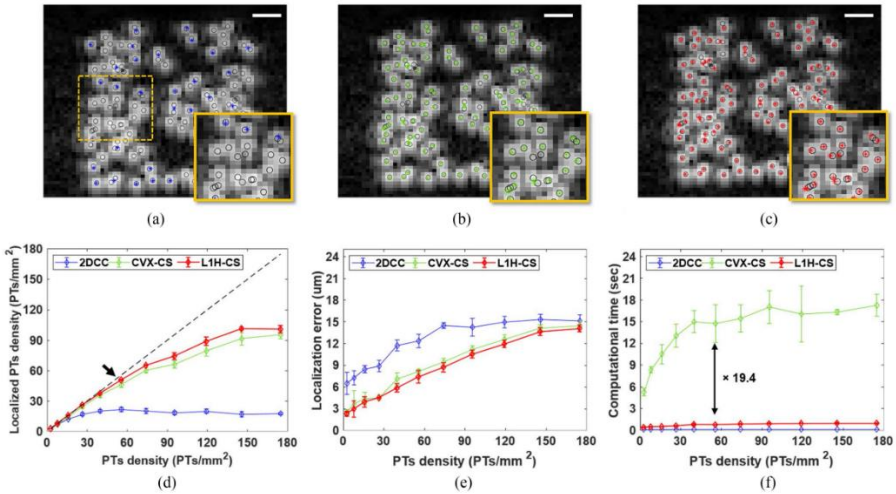


### D. In Vivo Mouse and Zebrafish Super-Resolution Ultrasound Imaging Using 1-homotopy Based Compressed Sensing Algorithm

In SRUS images of mouse tumours, the vessel sizes were measured to be 25.68 μm in profile 1, and the distances between adjacent vessels were measured to be 109.9 and 109.01 μm in profiles 2 and 3, respectively. The smallest vessel size is 22.2 μm by SRUS imaging. Considering the half wavelength of 25 MHz ultrasound the diffraction limit was overcome by L1H-CS based SRUS imaging.

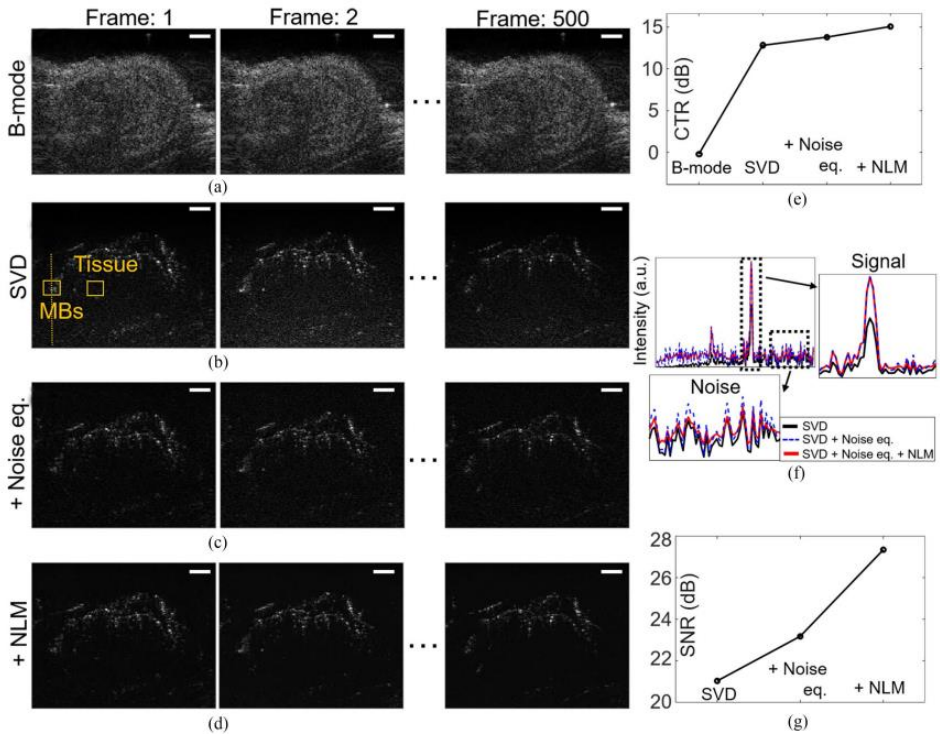

# Conclusion

In conclusion, we described the L1H-CS based SRUS imaging technique that could reduce computational time and acquisition time or significantly improve SRUS image quality with some expenses of post-processing cost. In the simulation, we confirmed that a minimum distinguishable distance of PTs was 27.5 μm, and efficient localization of PTs compared to a conventional localization technique. By in vivo mouse imaging, the minimum detectable blood vessel size in a mouse kidney was measured to be 22 μm, which confirms the sub-diffraction limit capability of L1H-CS. Based on results both in simulation and in vivo experiments, the proposed algorithm significantly improves SRUS image quality and data acquisition time. These results demonstrate that the L1H-CS-based SRUS imaging technique has the potential to examine microvasculature with reduced acquisition and reconstruction time to acquire enhanced SRUS image quality, which may be necessary to translate into clinics. Results demonstrate that the SRUS imaging technique could be substantially improved by applying L1H-CS algorithm for the localization of high-density MBs, suggesting its potential as a faster SRUS imaging technique

# References


1) N. A. Geis, H. A. Katus, and R. Bekeredjian, “Microbubbles as a vehicle for gene and drug delivery: Current clinical implications and future perspectives,” Curr. Pharmaceut. Des., vol. 18, no. 15, pp. 2166–2183, 2012.

2) C.-Y. Ting et al., “Concurrent blood-brain barrier opening and local drug delivery using drug-carrying microbubbles and focused ultrasound for brain glioma treatment,” Biomaterials, vol. 33, no. 2, pp. 704–712, 2012.

3) F. Yan et al., “Paclitaxel-liposome–microbubble complexes as ultrasound triggered therapeutic drug delivery carriers,” J. Controlled Release, vol. 166, no. 3, pp. 246–255, 2013.

4) C. R. Anderson et al., “Ultrasound molecular imaging of tumor angiogenesis with an integrin targeted microbubble contrast agent,” Invest. Radiol., vol. 46, no. 4, 2011, Art. no. 215.

5) H. Zhang et al., “Ultrasound molecular imaging of tumor angiogenesis with a neuropilin-1-targeted microbubble,” Biomaterials, vol. 56, pp. 104–113, 2015

6) J. Foiret et al., “Ultrasound localization microscopy to image and assess microvasculature in a rat kidney,” Sci. Rep., vol. 7, no. 1, 2017, Art. no. 13662.